Synthesis, Chemical Characterization, and Bonding Analysis of the $[Ag\{Fe(CO)_4\}_2]^{3-}$, $[Ag_4\{\mu_2\text{-}Fe(CO)_4\}_4]^{4-}$, and $[Ag_5\{\mu_2\text{-}Fe(CO)_4\}_2\{\mu_3\text{-}Fe(CO)_4\}_2]^{3-}$ Cluster Anions. X-ray Structural Determination of $[NMe_3CH_2Ph]_4[Ag_4Fe_4(CO)_{16}]$ and $[NEt_4]_3[Ag_5Fe_4(CO)_{16}]$

Vincenzo G. Albano,[†] Fabrizio Azzaroni,[‡] Maria Carmela Iapalucci,[‡] Giuliano Longoni,*[,‡] Magda Monari,*[,†] Suzanne Mulley,[§] Davide M. Proserpio,[§] and Angelo Sironi[§]

Dipartimento di Chimica "G. Ciamician", via F. Selmi 2, 40126 Bologna, Italy, Dipartimento di Chimica Fisica ed Inorganica, viale Risorgimento 4, 40136 Bologna, Italy, and Istituto di Chimica Strutturistica Inorganica, via G. Venezian 21, 20133 Milano, Italy

Received March 30, 1994[⊗]

The new $[Ag\{Fe(CO)_4\}_2]^{3-}$, $[Ag_4\{\mu_2\text{-}Fe(CO)_4\}_4]^{4-}$, and $[Ag_5\{\mu_2\text{-}Fe(CO)_4\}_2\{\mu_3\text{-}Fe(CO)_4\}_2]^{3-}$ cluster anions have been selectively obtained by reaction of $AgBF_4$ or $AgNO_3$ with $Na_2[Fe(CO)_4]\cdot x$THF in tetrahydrofuran and/or acetonitrile solutions in 0.5, 1, and 1.25 molar ratios, respectively. $[Ag_5\{\mu_2\text{-}Fe(CO)_4\}_2\{\mu_3\text{-}Fe(CO)_4\}_2]^{3-}$ has been isolated as a tetrasubstituted ammonium or phosphonium salt, by metathesis in methanol with the corresponding halides, and crystallized as either the $[NMe_3CH_2Ph]^+$ or $[N(PPh_3)_2]^+$ salt from acetone-isopropyl alcohol and acetonitrile-isopropyl ether mixtures, respectively. Neither the $[Ag\{Fe(CO)_4\}_2]^{3-}$ nor the $[Ag_4\{\mu_2\text{-}Fe(CO)_4\}_4]^{4-}$ anion could be isolated as an ammonium salt directly by metathesis, owing to the sensitivity of these ions to protic solvents. Their salts have been obtained indirectly by reaction of metathesized $[Ag_5\{\mu_2\text{-}Fe(CO)_4\}_2\{\mu_3\text{-}Fe(CO)_4\}_2]^{3-}$ salts with $Na_2[Fe(CO)_4]\cdot x$THF in THF, and crystallized by layering with toluene. The structures of $[NMe_3CH_2Ph]_4[Ag_4\{\mu_2\text{-}Fe(CO)_4\}_4]$ and $[NEt_4]_3[Ag_5\{\mu_2\text{-}Fe(CO)_4\}_2\{\mu_3\text{-}Fe(CO)_4\}_2]$ have been determined by X-ray diffraction studies. $[NMe_3CH_2Ph]_4[Ag_4\{\mu_2\text{-}Fe(CO)_4\}_4]$ is monoclinic, space group $P2_1/n$ (No. 14), with a = 11.419(4) Å, b = 29.714(5) Å, c=19.227(3) Å, and Z = 4 while $[NEt_4]_3[Ag_5\{\mu_2\text{-}Fe(CO)_4\}_2\{\mu_3\text{-}Fe(CO)_4\}_2]$ is tetragonal, space group $P4_2/mnm$ (No. 136), with a = 14.004(1) Å, c = 14.278(1) Å, and Z = 2. The $[Ag_4\{\mu_2\text{-}Fe(CO)_4\}_4]^{4-}$ and $[Ag_5\{\mu_2\text{-}Fe(CO)_4\}_2\{\mu_3\text{-}Fe(CO)_4\}_2]^{3-}$ anions both display an almost planar metal atom frame. The molecular structure of the $[Ag_4\{\mu_2\text{-}Fe(CO)_4\}_4]^{4-}$ anion consists of an Ag_4 square, spanned on all the edges by $Fe(CO)_4$ groups, the iron atoms describing a square of frequency 2 with the central atom missing. The idealized molecular symmetry is D_{4h}. The structure of the corresponding $[Ag_5\{\mu_2\text{-}Fe(CO)_4\}_2\{\mu_3\text{-}Fe(CO)_4\}_2]^{3-}$ conforms exactly to a rhombus of frequency 2; the vertices are occupied by the four iron atoms, whereas silver atoms are located in the middle of each edge and in the center of the rhombus. The electron counts of these clusters have been rationalized by extended Hückel molecular orbital calculations and their chemistry has been interpreted on the basis of isolobal analogies.

Introduction

In a previous paper we described the synthesis and characterization of the $[Ag_{13}\{Fe(CO)_4\}_8]^{4-}$ paramagnetic anion,[1] which was almost quantitatively obtained on reaction of $Na_2[Fe(CO)_4]\cdot x$THF in tetrahydrofuran or acetonitrile with ca. 1.6 mol of $AgBF_4$ or $AgNO_3$. During the preparation of this species the intermediate formation of several other diamagnetic carbonyl species was monitored by IR. This, as well as recognition that homo- and heterometallic silver clusters were exceedingly rare,[2-4] prompted a systematic investigation of the above reaction.

We now report the synthesis and characterization of the $[Ag\{Fe(CO)_4\}_2]^{3-}$, $[Ag_4\{\mu_2\text{-}Fe(CO)_4\}_4]^{4-}$, and $[Ag_5\{\mu_2\text{-}Fe(CO)_4\}_2\{\mu_3\text{-}Fe(CO)_4\}_2]^{3-}$ cluster anions, which represent the initial products of the sequential condensation of silver and $[Fe(CO)_4]^{2-}$ ions.

A $[Cu_5\{\mu_2\text{-}Fe(CO)_4\}_2\{\mu_3\text{-}Fe(CO)_4\}_2]^{3-}$ species, with a structure identical to that of $[Ag_5\{\mu_2\text{-}Fe(CO)_4\}_2\{\mu_3\text{-}Fe(CO)_4\}_2]^{3-}$, as well as a $[Cu_3\{\mu_2\text{-}Fe(CO)_4\}_3]^{3-}$ trianion, has previously been isolated from the related reaction of CuCl with $[Fe(CO)_4]^{2-}$.[5] The difference in the condensation sequence of copper and silver prompted a reinvestigation of the reaction of CuCl with $[Fe(CO)_4]^{2-}$ ions, which pointed out the initial formation of a $[Cu\{Fe(CO)_4\}_2]^{3-}$ species, corresponding to $[Ag\{Fe(CO)_4\}_2]^{3-}$. The possible reasons for the observed growth paths of the Cu-Fe and Ag-Fe clusters are discussed with the support of EHMO calculations and isolobal analogies.[6]

A preliminary report on the chemistry of Ag-Fe bimetallic clusters has already appeared.[7]

Results and Discussion

1. Synthesis, Spectroscopic and Chemical Characterization of the $[Ag\{Fe(CO)_4\}_2]^{3-}$, $[Ag_4\{\mu_2\text{-}Fe(CO)_4\}_4]^{4-}$, and $[Ag_5\{\mu_2\text{-}Fe(CO)_4\}_2\{\mu_3\text{-}Fe(CO)_4\}_2]^{3-}$ Cluster Anions. As previously reported,[1,7] the addition of $AgBF_4$ or $AgNO_3$ to $Na_2[Fe(CO)_4]\cdot x$THF in a tetrahydrofuran (THF) suspension or

[†] Dipartimento di Chimica "G. Ciamician".
[‡] Dipartimento di Chimica Fisica ed Inorganica.
[§] Istituto di Chimica Strutturistica Inorganica.
[⊗] Abstract published in *Advance ACS Abstracts,* September 15, 1994.

(1) Albano, V. G.; Grossi, L.; Longoni, G.; Monari, M.;Mulley, S.; Sironi, A.; *J. Am. Chem. Soc.* **1992**, *114*, 5708.
(2) Noltes,J. G.; van Koten, G. In *Comprehensive Organometallic Chemistry*; Wilkinson, G., Stone, F. G. A., Abel, E. W., Eds.; Pergamon Press: Oxford, England, 1981; Vol 2, p 709.
(3) Salter, I. D. *Adv. Organomet. Chem.* **1989**, *29*, 249.
(4) Mingos, D. M. P.; May, A. S. In *Chemistry of Metal Cluster Complexes*; Shriver, D. F., Kaesz, H. D., Adams, R. D., Eds.; VCH: Weinheim, Germany, 1990.
(5) Doyle, G.; Eriksen, K. A.; Van Engen, D. *J. Am. Chem. Soc.* **1985**, *107*, 7914.
(6) Hoffmann, R.; *Angew. Chem., Int. Ed. Engl.* **1982**, *21*, 711.
(7) Albano, V. G.; Azzaroni, F.; Iapalucci, M. C.; Longoni, G.; Monari, M.; Mulley, S. In *Chemical Processes in Inorganic Materials: Metal and Semiconductor Cluster and Colloids*; Persans, P. D., Bradley, J. S., Chianelli, R. R., Schmid, G. Eds.; Materials Research Society Symposia Proceedings 272; Materials Research Society: New York, 1992; p 115.

0020-1669/94/1333-5320$04.50/0

acetonitrile solution progressively yields new carbonyl species showing infrared carbonyl absorptions with increasingly higher frequencies. The first detectable reaction product, namely $[Ag\{Fe(CO)_4\}_2]^{3-}$, is obtained along with minor amounts of $[HFe(CO)_4]^-$ on addition of ca. 0.4−0.5 mol of silver salt per mole of $Na_2[Fe(CO)_4]\cdot x$THF, according to reaction 1. All

$$2[Fe(CO)_4]^{2-} + Ag^+ \rightarrow [Ag\{Fe(CO)_4\}_2]^{3-} \quad (1)$$

attempts to isolate the $[Ag\{Fe(CO)_4\}_2]^{3-}$ trianion from these reaction mixtures by metathesis with tetrasubstituted ammonium or phosphonium halides in methanol resulted in the separation of precipitates consisting mainly of mixtures of the corresponding $[Ag_5\{\mu_2\text{-}Fe(CO)_4\}_2\{\mu_3\text{-}Fe(CO)_4\}_2]^{3-}$ and $[HFe(CO)_4]^-$ salts, owing to the occurrence of the overall reaction 2. Spectroscopically pure microcrystalline samples of $[N(PPh_3)_2]_3[Ag\{Fe(CO)_4\}_2]$ and $[Na(15\text{-crown-}5)]_3[Ag\{Fe(CO)_4\}_2]$ have been obtained from preformed $[N(PPh_3)_2]_4[Ag_4\{\mu_2\text{-}Fe(CO)_4\}_4]$ by reaction with $Na_2[Fe(CO)_4]\cdot x$THF according to reaction 3, or by performing reaction 1 in the presence of 15-crown-5. In both cases the respective $[Ag\{Fe(CO)_4\}_2]^{3-}$ salts separate out from the THF solution due to their low solubility in this solvent.

$$5[Ag\{Fe(CO)_4\}_2]^{3-} + 6H_2O \rightarrow [Ag_5\{\mu_2\text{-}Fe(CO)_4\}_2\{\mu_3\text{-}Fe(CO)_4\}_2]^{3-} + 6[HFe(CO)_4]^- + 6OH^- \quad (2)$$

$$[Ag_4\{\mu_2\text{-}Fe(CO)_4\}_4]^{4-} + 4[Fe(CO)_4]^{2-} \rightarrow 4[Ag\{Fe(CO)_4\}_2]^{3-} \quad (3)$$

The $[Ag\{Fe(CO)_4\}_2]^{3-}$ salts are almost colorless and show infrared carbonyl absorptions in acetonitrile at 1883 (ms) and 1799 (s, broad) cm^{-1}. The IR pattern is similar to that of the related $[M\{Co(CO)_4\}_2]^-$ (M = Cu, Ag, Au)[8,9] and $[M\{Fe(CO)_4\}_2]^{2-}$ (M = Zn, Cd, Hg) linear clusters.[10,11] The increased anionic charge in the above series of compounds is reflected by a lowering of ca. 90 cm^{-1} on going from the mono- to the dianionic species and ca. 55 cm^{-1} on going from the dianion to the trianionic $[Ag\{Fe(CO)_4\}_2]^{3-}$ compound.

Reaction of $[Ag\{Fe(CO)_4\}_2]^{3-}$ with 1 mol of silver salt results in the quantitative formation of $[Ag_4\{\mu_2\text{-}Fe(CO)_4\}_4]^{4-}$, according to eq 4. Solutions of this compound are more conveniently

$$2[Ag\{Fe(CO)_4\}_2]^{3-} + 2Ag^+ \rightarrow [Ag_4\{\mu_2\text{-}Fe(CO)_4\}_4]^{4-} \quad (4)$$

and readily obtained by reacting $Na_2[Fe(CO)_4]\cdot x$THF and $AgNO_3$ in acetonitrile in a 1:1 molar ratio, as a result of the consecutive occurrence of reactions 1 and 4. As with the $[Ag\{Fe(CO)_4\}_2]^{3-}$ trianion, metathesis in methanol of $Na_4[Ag_4\{\mu_2\text{-}Fe(CO)_4\}_4]\cdot x$THF with tetrasubstituted ammonium or phosphonium halides results in the precipitation of a mixture of the corresponding $[Ag_5\{\mu_2\text{-}Fe(CO)_4\}_2\{\mu_3\text{-}Fe(CO)_4\}_2]^{3-}$ and $[HFe(CO)_4]^-$ salts, owing to reaction 5. The $[Ag_4(\mu_2\text{-}Fe(CO)_4\}_4]^{4-}$ anion has been isolated in the solid state in good yields (60−70%) with several counterions, e.g. $[NEt_4]^+$, $[NMe_3CH_2Ph]^+$, and $[N(PPh_3)_2]^+$, by performing reaction 6 on the corresponding $[Ag_5\{\mu_2\text{-}Fe(CO)_4\}_2\{\mu_3\text{-}Fe(CO)_4\}_2]^{3-}$ salts in THF, and by then layering toluene on the resulting reaction solution.

$$5[Ag_4\{\mu_2\text{-}Fe(CO)_4\}_4]^{4-} + 4H_2O \rightarrow 4[Ag_5\{\mu_2\text{-}Fe(CO)_4\}_2\{\mu_3\text{-}Fe(CO)_4\}_2]^{3-} + 4[HFe(CO)_4]^- + 4OH^- \quad (5)$$

$$4[Ag_5\{\mu_2\text{-}Fe(CO)_4\}_2\{\mu_3\text{-}Fe(CO)_4\}_2]^{3-} + 4[Fe(CO)_4]^{2-} \rightarrow 5[Ag_4\{\mu_2\text{-}Fe(CO)_4\}_4]^{4-} \quad (6)$$

The $[Ag_4\{\mu_2\text{-}Fe(CO)_4\}_4]^{4-}$ salts are pale yellow in color and show infrared carbonyl absorptions in acetonitrile at 1930 (ms) and 1851 (s) cm^{-1}. Their elemental analyses pointed toward an empirical formula $[Ag\{Fe(CO)_4\}]^-$; however, their infrared absorption frequencies were rather different from those of the previously reported $[Cu_3(\mu_2\text{-}Fe(CO)_4\}_3]^{3-}$.[5] An X-ray structural determination revealed a tetrameric $[Ag_4\{\mu_2\text{-}Fe(CO)_4\}_4]^{4-}$ stoichiometry (*see later*). Isolation of a tetramer of $[AgFe(CO)_4]^-$, rather than a trimer as for the $[CuFe(CO)_4]^-$ congener, may originate from several miscellaneous factors, e.g. thermodynamic or kinetic reasons as well as packing forces. It appeared, for instance, possible that scarcely coordinating or noncoordinating counterions of Ag^+ such as NO_3^- and BF_4^- could play some role in driving reaction 1 toward the formation of $[Ag\{Fe(CO)_4\}_2]^{3-}$ and, hence, to $[Ag_4\{\mu_2\text{-}Fe(CO)_4\}_4]^{4-}$ through reaction 4, rather than directly to $[Ag_3(\mu_2\text{-}Fe(CO)_4\}_3]^{3-}$. Indeed, in the case of the Cu−Fe clusters, only Cu(I) salts with a coordinating counterion (Cl^-, Br^-) have been used.[5] However, AgCl afforded the same products as those obtained with $AgNO_3$ and $AgBF_4$, although less conveniently owing to concomitant formation of silver metal and oxidized iron carbonyl anions. Moreover, a reinvestigation of the reaction of $[Fe(CO)_4]^{2-}$ with CuCl in a ca. 2−2.2 molar ratio disclosed the existence of a $[Cu\{Fe(CO)_4\}_2]^{3-}$ species (ν_{CO} in acetonitrile at 1884 (ms) and 1807 (s) cm^{-1}) corresponding to $[Ag\{Fe(CO)_4\}_2]^{3-}$. Nevertheless, the former gives rise to $[Cu_3(\mu_2\text{-}Fe(CO)_4\}_3]^{3-}$ by reaction with additional CuCl, rather than $[Cu_4(\mu_2\text{-}Fe(CO)_4\}_4]^{4-}$. The trimeric nature of this reaction product has also been confirmed through molecular weight determinations *via* density and X-ray unit cell measurements on its $[NEt_4]^+$, $[NMe_3CH_2Ph]^+$ and $[NBu_4]^+$ salts. Therefore, both kinetic factors and packing forces can be ruled out as possible reasons of the observed differences in the chemistry of Ag−Fe and Cu−Fe clusters.

As shown in eq 7, the reaction of $[Ag_4\{\mu_2\text{-}Fe(CO)_4\}_4]^{4-}$ with an equimolar amount of Ag^+ ion affords the $[Ag_5\{\mu_2\text{-}Fe(CO)_4\}_2\{\mu_3\text{-}Fe(CO)_4\}_2]^{3-}$ trianion quantitatively. This, however, was more conveniently obtained by the direct reaction of $Na_2[Fe(CO)_4]\cdot x$THF with ca. 1.2−1.3 mol of $AgNO_3$ in acetonitrile, as a result of the sequence of reactions 1, 4, and 7. In contrast to both $[Ag\{Fe(CO)_4\}_2]^{3-}$ and $[Ag_4\{\mu_2\text{-}Fe(CO)_4\}_4]^{4-}$, the $[Ag_5\{\mu_2\text{-}Fe(CO)_4\}_2\{\mu_3\text{-}Fe(CO)_4\}_2]^{3-}$ trianion is not sensitive to humidity and has been isolated in the solid state with several tetrasubstituted ammonium and phosphonium salts by metathesis in methanol with the corresponding halides. These salts show infrared carbonyl absorptions in acetonitrile solution at 1949 (ms) and 1979 (s) cm^{-1}.

$$[Ag_4\{\mu_2\text{-}Fe(CO)_4\}_4]^{4-} + Ag^+ \rightarrow [Ag_5\{\mu_2\text{-}Fe(CO)_4\}_2\{\mu_3\text{-}Fe(CO)_4\}_2]^{3-} \quad (7)$$

The further addition of silver(I) salts to a solution of $[Ag_5\{\mu_2\text{-}Fe(CO)_4\}_2\{\mu_3\text{-}Fe(CO)_4\}_2]^{3-}$ causes the progressive appearance of new infrared carbonyl absorptions at 1970 and 1885 cm^{-1}, which are subsequently substituted on further addition of Ag^+ by the absorptions of $[Ag_{13}\{\mu_3\text{-}Fe(CO)_4\}_8]^{4-}$ (1980 (s) and 1880 (m) cm^{-1})[1] and $[Ag_{13}\{\mu_3\text{-}Fe(CO)_4\}_8]^{3-}$ (2000 (s) and

(8) Chini, P.; Martinengo, S.; Longoni, G. *Gazz. Chim. Ital.* **1975**, *105*, 203.
(9) Uson, R.; Laguna, A.; Laguna, M.; Jones, P. G.; Sheldrick, G. *J. Chem. Soc. Dalton Trans.* **1981**, 366.
(10) Sosinsky, B.; Shong, R. G.; Fitzgerald, B. J.; Nozem, N.; O'Rourke, C.; *Inorg. Chem.* **1983**, *22*, 3124.
(11) Alvarez, S.; Ferrer, M.; Reina, R.; Rossell, O.; Seco, M.; Solans, X. *J. Organomet. Chem.* **1989**, *377*, 291.

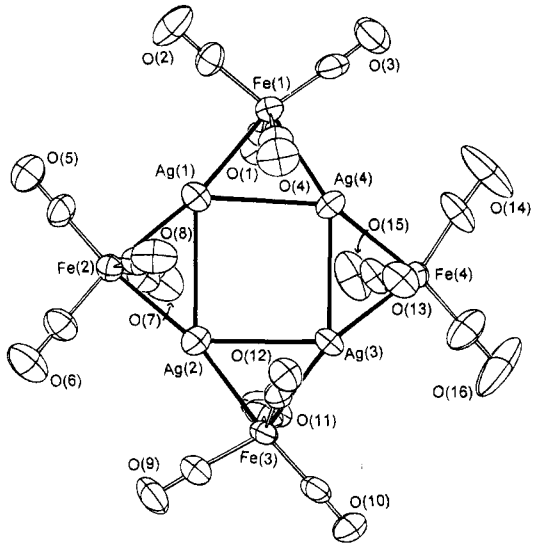

Figure 1. ORTEP drawing of the $[Ag_4\{\mu_2\text{-}Fe(CO)_4\}_4]^{4-}$ tetraanion showing the idealized D_{4h} molecular symmetry. C atoms of the CO groups bear the same numbering as the O atoms.

1915 (m) cm^{-1}).[12] The carbonyl absorptions at 1970 and 1885 cm^{-1} are probably attributable to a $[Ag_6\{Fe(CO)_4\}_4]^{2-}$ species corresponding to the previously reported $[Cu_6\{\mu_3\text{-}Fe(CO)_4\}_4]^{2-}$ dianion.[13]

2. Structural Characterization of $[NMe_3CH_2Ph]_4[Ag_4\{\mu_2\text{-}Fe(CO)_4\}_4]$ and $[NEt_4]_3[Ag_5\{\mu_2\text{-}Fe(CO)_4\}_2\{\mu_3\text{-}Fe(CO)_4\}_2]$. The structure of $[Ag_4\{\mu_2\text{-}Fe(CO)_4\}_4]^{4-}$, shown in Figure 1, contains an Ag_4Fe_4 planar cluster consisting of an idealized square of silver atoms (average Ag−Ag distance 3.149 Å) surrounded by four edge-bridging $Fe(CO)_4$ groups (average Fe−Ag distance 2.581 Å). The resulting metal atom aggregate is a second-order square of iron atoms circumscribing a slightly reentrant square of silver atoms. The $Fe(CO)_4$ fragments adopt a C_{2v} conformation and the anion as a whole can be attributed an idealized D_{4h} symmetry. It is significant that the weak Ag−Ag interactions are distributed over the range 3.036−3.334(1) Å, while the stronger Ag−Fe bonds span the narrow interval 2.574−2.600(2) Å. The Ag−Ag interactions, though weak, are attractive, as indicated by the inward bending of the Fe−Ag−Fe linear sequences (average angle 165.4°). The $Fe(CO)_4$ groups are six-connected and the coordination geometry at the Fe atom can be described as distorted octahedral, although the only angle reminiscent of this coordination is that defined by the in-plane CO groups [average C(equatorial)−Ag−C(equatorial) angle 103.0°]. The angle formed by the axial ligands [average 135.4°] is too far from the ideal one (180°) and can not be explained in terms of mere optimization of intraligand contacts. A comparison of the Ag···CO distances for axial and equatorial carbonyl ligands [average values Ag···C(axial) 2.66 Å and Ag···C(equatorial) 3.14 Å] gives a good indication in favor of attractive Ag···C(axial) interactions. This evidence is confirmed by some deviation from linearity of these ligands [average angles Fe−C−O(axial) 174.5°, Fe−C−O(equatorial) 177.9°]. The geometry of $[Ag_4\{\mu_2\text{-}Fe(CO)_4\}_4]^{4-}$ is strictly comparable to that of the neutral and isoelectronic $[Ag_4\{\mu_2\text{-}Co(CO)_4\}_4]$,[14] in spite of the differences in charge and crystal organization. The main difference is a greater regularity of the Ag_4 square in the latter [Ag−Ag(average) 3.02 Å], motivated by the precise C_{2h} symmetry adopted by the molecule in the crystal.

Table 1. Selected Bond Lengths (Å) and Angles (deg) for $[Ag_4\{\mu_2\text{-}Fe(CO)_4\}_4]^{4-}$

Ag(1)−Ag(2)	3.334(1)	Fe(1)−C(1)	1.77(1)
Ag(2)−Ag(3)	3.036(1)	C(1)−O(1)	1.18(1)
Ag(1)−Ag(4)	3.050(1)	Fe(1)−C(2)	1.76(1)
Ag(3)−Ag(4)	3.175(1)	C(2)−O(2)	1.16(2)
Ag(1)−Fe(1)	2.592(2)	Fe(1)−C(3)	1.75(1)
Ag(4)−Fe(1)	2.581(2)	C(3)−O(3)	1.17(2)
Ag(1)−Fe(2)	2.574(2)	Fe(1)−C(4)	1.77(1)
Ag(2)−Fe(2)	2.577(2)	C(4)−O(4)	1.16(1)
Ag(2)−Fe(3)	2.581(2)	Fe(2)−C(5)	1.74(1)
Ag(3)−Fe(3)	2.600(2)	C(5)−O(5)	1.16(2)
Ag(3)−Fe(4)	2.577(2)	Fe(2)−C(6)	1.74(1)
Ag(4)−Fe(4)	2.570(2)	C(6)−O(6)	1.17(2)
Fe(2)−C(7)	1.76(1)	Fe(3)−C(10)	1.75(1)
C(7)−O(7)	1.16(2)	C(10)−O(10)	1.16(2)
Fe(2)−C(8)	1.78(1)	Fe(3)−C(11)	1.78(1)
C(8)−O(8)	1.17(1)	C(11)−O(11)	1.16(1)
Fe(3)−C(9)	1.76(1)	Fe(3)−C(12)	1.75(1)
C(9)−O(9)	1.16(2)	C(12)−O(12)	1.19(2)
Fe(4)−C(13)	1.76(1)	Fe(4)−C(15)	1.75(1)
C(13)−O(13)	1.17(1)	C(15)−O(15)	1.17(2)
Fe(4)−C(14)	1.73(1)	Fe(4)−C(16)	1.73(1)
C(14)−O(14)	1.15(2)	C(16)−O(16)	1.15(2)
Ag(1)···C(1)	2.64	Ag(3)···C(11)	2.58
Ag(1)···C(2)	3.17	Ag(3)···C(12)	2.57
Ag(1)···C(4)	2.73	Ag(3)···C(13)	2.63
Ag(1)···C(7)	2.69	Ag(3)···C(10)	3.41
Ag(1)···C(8)	2.61	Ag(3)···C(15)	2.61
Ag(1)···C(5)	3.11	Ag(3)···C(16)	3.24
Ag(2)···C(7)	2.58	Ag(4)···C(1)	2.72
Ag(2)···C(8)	2.69	Ag(4)···C(4)	2.56
Ag(2)···C(9)	2.97	Ag(4)···C(3)	3.15
Ag(2)···C(6)	3.10	Ag(4)···C(13)	2.76
Ag(2)···C(11)	2.74	Ag(4)···C(14)	2.96
Ag(2)···C(12)	2.77	Ag(4)···C(15)	2.63

Ag(1)−Fe(1)−Ag(4)	72.2(1)	Ag(2)−Ag(1)−Ag(4)	87.4(1)
Ag(1)−Fe(2)−Ag(2)	80.7(1)	Ag(1)−Ag(4)−Ag(3)	92.3(1)
Ag(2)−Fe(3)−Ag(3)	71.7(1)	Ag(4)−Ag(3)−Ag(2)	90.6(1)
Ag(3)−Fe(4)−Ag(4)	76.2(1)	Ag(3)−Ag(2)−Ag(1)	89.5(1)
Fe(1)−Ag(1)−Fe(2)	169.3(1)	Fe(1)−C(1)−O(1)	176(1)
Fe(2)−Ag(2)−Fe(3)	166.7(1)	Fe(1)−C(2)−O(2)	178(1)
Fe(3)−Ag(3)−Fe(4)	164.0(1)	Fe(1)−C(3)−O(3)	176(1)
Fe(4)−Ag(4)−Fe(1)	161.6(1)	Fe(1)−C(4)−O(4)	172(1)
C(1)−Fe(1)−C(4)	136.9(6)	Fe(2)−C(5)−O(5)	178(1)
C(7)−Fe(2)−C(8)	132.9(6)	Fe(2)−C(6)−O(6)	179(1)
C(11)−Fe(3)−C(12)	135.3(6)	Fe(2)−C(7)−O(7)	173(1)
C(13)−Fe(4)−C(15)	136.5(6)	Fe(2)−C(8)−O(8)	178(1)
C(2)−Fe(1)−C(3)	105.3(6)	Fe(3)−C(9)−O(9)	179(1)
C(5)−Fe(2)−C(6)	100.1(6)	Fe(3)−C(10)−O(10)	177(1)
C(9)−Fe(3)−C(10)	102.7(6)	Fe(3)−C(11)−O(11)	171(1)
C(14)−Fe(4)−C(16)	103.9(7)	Fe(3)−C(12)−O(12)	173(1)
Fe(4)−C(13)−O(13)	173(1)	Fe(4)−C(14)−O(14)	177(1)
Fe(4)−C(15)−O(15)	173(1)	Fe(4)−C(16)−O(16)	179(2)

The structure of $[NEt_4]_3[Ag_5\{\mu_2\text{-}Fe(CO)_4\}_2\{\mu_3\text{-}Fe(CO)_4\}_2]$, shown in Figure 2, contains a planar cluster of nine metal atoms packed in a rhombus. The Fe atoms define the vertices and the silver atoms are placed almost midway along the edges and in the center. Both the idealized and crystallographic symmetry of the anion is D_{2h}, in spite of the unfavorable stoichiometry of the salt. The silver atoms define a bow tie with four equivalent atoms at the corners and a unique central atom. The latter is six-connnected to four silver and two iron atoms and exhibits bonding distances both from the silver and the iron [Ag(1)−Ag 2.795(1) Å and Ag(1)−Fe 2.727(1) Å]. The Ag−Ag value is shorter than the distance in the bulk metal (2.88 Å).[15] The corner atoms are four-connected, with two Ag−Ag and two Ag−Fe interactions. The Ag−Ag distance bridged by the $Fe(CO)_4$ group [3.017(1) Å] is longer than the values above,

(12) Albano,V. G.; Calderoni,F.; Iapalucci, M. C.; Longoni, G.; Monari, M.; Zanello, P. Manuscript in preparation
(13) Doyle, G.; Eriksen, K. A.; Van Engen, D. *J. Am. Chem. Soc.* **1986**, *108*, 445.
(14) Klufers, P. *Z. Krystallogr.* **1984**, *166*, 143.

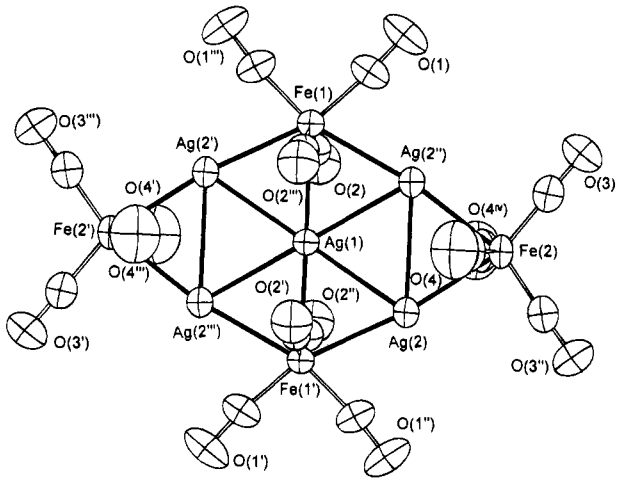

Figure 2. ORTEP drawing of the $[Ag_5\{\mu_2\text{-}Fe(CO)_4\}_2\{\mu_3\text{-}Fe(CO)_4\}_2]^{3-}$ trianion conforming to a D_{2h} symmetry imposed by the crystal packing. Symmetry related atoms: (I) = $-x, -y, -z$; (II) = y, x, z; (III) = $-y, -x, -z$; (IV) = $y, x, -z$. C atoms of the CO groups bear the same numbering as the O atoms.

and in accordance with those found in $[Ag_4\{\mu_2\text{-}Fe(CO)_4\}_4]^{4-}$ (see preceding section). The $Fe(CO)_4$ groups form two independent pairs, both conform to a precise C_{2v} symmetry but differ in the number of iron-silver interactions. Fe(1) and Fe(1′) are three-connected to the silver atoms resulting in a distorted pentagonal bipyramidal coordination. Fe(2) and Fe(2′) are two-connected and realize a more conventional octahedral-like coordination, similar to that found in $[Ag_4\{\mu_2\text{-}Fe(CO)_4\}_4]^{4-}$. The differences in coordination numbers are reflected in the Fe–Ag distances. The actual values are 2.585(1) Å for the six-coordinate Fe(2) and 2.650(1) and 2.727(1) Å for the seven-coordinate Fe(1). Another significant difference between the two kinds of $Fe(CO)_4$ groups is observed in the degree of tetrahedral deformation of the CO ligands. While the axial groups show the expected leaning toward the silver atoms (see preceding section) equal for the two independent sets [C(2)–Fe(1)–C(2‴) 141.4(6)°; C(4)–Fe(2)–C(4^{IV}) 141.2(7)°] the opening of the angle between the equatorial ligands is quite different [C(1)–Fe(1)–C(1‴) 94.4(6)°; C(3)–Fe(2)–C(3″) 107.3(5)°]. Furthermore, the seven-coordinate Fe(1) have both axial and equatorial ligands in close contact with the silver atoms [C(2)···Ag(1) 2.72 Å; C(1)···Ag(2″) 2.64 Å], while only the axial ligands show this interaction for the six-coordinate Fe(2) atoms [C(4)···Ag(2) 2.70 Å; C(3)···Ag(2″) 3.13 Å]. Significantly, these contacts induce some bending of the ligands involved (see Table 2), strengthening the evidence of their slightly bonded nature. All the structural features discussed for $[Ag_5\{\mu_2\text{-}Fe(CO)_4\}_2\{\mu_3\text{-}Fe(CO)_4\}_2]^{3-}$ are strictly equivalent to those reported for the copper analogue $[Cu_5Fe_4(CO)_{16}]^{3-}$[5] crystallized with the same cation. Finally, it should be noted that the C(axial)–Fe–C(axial) angles show a clear dependence on the charge present in the molecules [135.4° in $[Ag_4\{\mu_2\text{-}Fe(CO)_4\}_4]^{4-}$, 141.3° in $[Ag_5\{\mu_2\text{-}Fe(CO)_4\}_2\{\mu_3\text{-}Fe(CO)_4\}_2]^{3-}$, and 145.8° in $[Ag_4\{\mu_2\text{-}Co(CO)_4\}_4]$. This seems to be due to the contribution of the Ag···CO interactions to the charge equalization mechanism throughout the molecules.

3. Bonding Analysis of the $[Ag_4\{\mu_2\text{-}Fe(CO)_4\}_4]^{4-}$ and $[Ag_5\{\mu_2\text{-}Fe(CO)_4\}_2\{\mu_3\text{-}Fe(CO)_4\}_2]^{3-}$ Cluster Anions. To rationalize the chemistry of the title Ag–Fe clusters and gain some understanding of the electron counting and the bonding in $[Ag_4\{\mu_2\text{-}Fe(CO)_4\}_4]^{4-}$ and $[Ag_5\{\mu_2\text{-}Fe(CO)_4\}_2\{\mu_3\text{-}Fe(CO)_4\}_2]^{3-}$, it is of primary importance to analyze the donor properties of the $Fe(CO)_4$ fragment. The shape and the number of out-pointing hybrid orbitals of a metal carbonyl fragment can be varied by changing the geometric disposition of the carbonyl ligands. A d^8 $M(CO)_4$ fragment may behave as follows: (i) as a one-orbital fragment (zero-electron donor) if derived from a trigonal bipyramid (**I**), as in $[Fe_3(CO)_9H\{\mu_3\text{-}P\rightarrow Fe(CO)_4\}]^{2-}$;[16] (ii) as a two-orbital fragment (two-electron donor) if derived from an octahedron, as in $[Ru_3(CO)_{12}]$ (**II**, coordinately-*cis*-divacant octahedron)[17] or in $[Ru(CO)_4]_n$ (**III**, coordinately-*trans*-divacant octahedron).[18] The presence of

Table 2. Selected Bond Lengths (Å) and Angles (deg) for $[Ag_5\{_2\text{-}Fe(CO)_4\}_2\{\mu_3\text{-}Fe(CO)_4\}_2]^{3-}$

Ag(1)–Ag(2)	2.795(1)	Fe(2)–C(3)	1.732(8)
Ag(2)–Ag(2^{II})	3.017(1)	C(3)–O(3)	1.21(1)
Ag(1)–Fe(1)	2.727(1)	Fe(2)–C(4)	1.748(8)
Ag(2)–Fe(2)	2.585(1)	C(4)–O(4)	1.17(1)
Ag(2)–Fe(1^{I})	2.650(1)	Ag(1)···C(2)	2.72
Fe(1)–C(1)	1.770(7)	Ag(2)···C(4)	2.70
C(1)–O(1)	1.16(1)	Ag(2)···C(1^{I})	2.96
Fe(1)–C(2)	1.772(7)	Ag(2)···C(1^{II})	2.64
C(2)–O(2)	1.16(1)	Ag(2)···C(3^{III})	3.13

Ag(2)–Fe(2)–Ag(2^{II})	71.4(1)	Fe(1)–C(1)–O(1)	173.4(8)
Ag(2)–Fe(1^{I})–Ag(1)	62.6(1)	Fe(1)–C(2)–O(2)	175.6(8)
Ag(2)–Ag(1)–Ag(2^{II})	65.3(1)	Fe(2)–C(3)–O(3)	179.3(7)
C(3)–Fe(2)–C(3^{II})	107.3(5)	Fe(2)–C(4)–O(4)	172.1(8)
C(1)–Fe(1)–C(1^{III})	94.4(6)	C(2)–Fe(1)–C(2^{III})	141.4(6)
C(4)–Fe(2)–C(4^{IV})	141.2(7)		

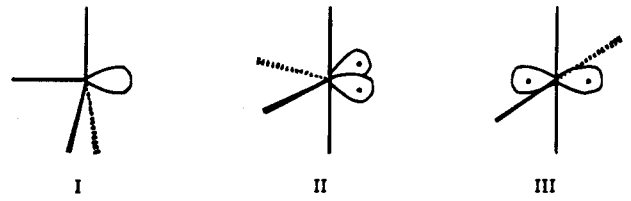

"nonbonding" *d* orbitals within the fragment leads to additional flexibility of their bonding capabilities, permitting higher coordination numbers. For instance, three-orbital–four-electron donor fragments are derived from one of the possible seven-vertex polyhedra,[6] such as **IV** (related to **II**) and **V** (related to **I**). Fragment **IV** is present in the structure of $[Ag_5\{\mu_2\text{-}Fe(CO)_4\}_2\{\mu_3\text{-}Fe(CO)_4\}_2]^{3-}$, while **V** is documented in the structures of $Ag_6Fe_3(CO)_{12}(HC(PPh_2)_3)$ and $[Ag_{12}(\mu_{12}\text{-}Ag)\{\mu_3\text{-}Fe(CO)_4\}_8]^{4-}$.[1,19]

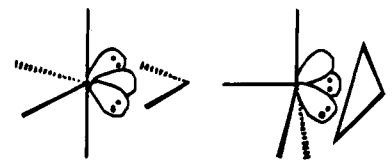

Therefore, the bonding capabilities of a metal carbonyl fragment should not be viewed as immutable, and its character may change in order to maximize its bonding interactions with the substrate.[20]

(15) Wells, A. F. In *Structural Inorganic Chemistry*, 5th ed.; Clarendon Press: Oxford, 1984; England, p 1288.

(16) Cané, M.;Iapalucci, M. C.; Longoni, G.; Demartin, F.; Grossi ,L.; *Mat. Chem. Phys.* **1991**, *29*, 395; for the purposes of electron bookkeeping, the $Fe(CO)_4$ fragment acts as a two-electron acceptor.

(17) Mason, R.; Rae, J. M. *J. Chem. Soc. A* **1968**, 778.

(18) Masciocchi, N.; Moret, M.; Cairati, P.; Ragaini, F.; Sironi, A. *J. Chem. Soc., Dalton Trans.* **1993**, 471. For the purposes of electron bookkeeping, the $Ru(CO)_4$ fragment acts as a two-electron donor.

(19) Briant, C. E.; Smith, R. G.; Mingos, D. M. P. *J. Chem. Soc., Chem. Commun.* **1984**, 586.

(20) Mingos, D. M. P. In *Inorganometallic Chemistry*; Fehlner, T. P., Ed.; Plenum Press: New York, 1992; p 179.

A common feature of the $Fe(CO)_4$ fragment in the solid state structure of its derivatives is a more or less pronounced departure from the idealized stereogeometries **I**−**V** owing to a bending of the carbonyl groups. This is particularly evident when $Fe(CO)_4$ is bound to late transition elements. For instance, the **I**-C_{3v} fragment in the linear $[Hg\{Fe(CO)_4\}_2]^{2-}$ presents the three equatorial carbonyls slightly bent toward the central Hg atom.[11] The μ_2-$Fe(CO)_4$ fragment is even more heavily distorted, for instance, the axial CO ligands of the *cis*-divacant octahedron (**II**) may bend toward the bonded metals and the iron environment then approaches that of the *cis*-(face)bicapped tetrahedron (**VI**), as in $[Ag_4\{\mu_2\text{-}Fe(CO)_4\}_4]^{4-}$. Similarily, in the coordinately *trans*-divacant octahedron (**III**), if the two pairs of *trans* CO ligands bend toward opposite bonded metals, the iron environment becomes a *trans*-(edge)bicapped tetrahedron (**VII**), as in $[(PPh_3)_2Cu]_2Fe(CO)_4$.[13]

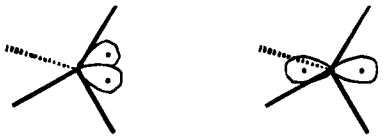

VI VII

An analogous tendency toward a tetrahedral disposition of the four CO ligands is also found in both the μ_3-$Fe(CO)_4$ (**IV**) and (**V**) fragments as documented respectively by $[M_5\{\mu_3\text{-}Fe(CO)_4\}_4]^{3-}$ (M = Cu,Ag) and $[Cu_6\{\mu_3\text{-}Fe(CO)_4\}_4]^{2-}$.[5,13] In the case of $[HPd_6\{\mu_3\text{-}Fe(CO)_4\}_6]^{3-}$, the leaning of the axial carbonyls toward Pd is so pronounced that these can be described as μ_2- and μ_3-bridging carbonyl groups.[21] In the latter, as shown by IR and ^{13}C NMR spectroscopy, these interactions are also retained in solution.[21,22]

Several explanations have been put forward to explain these distortions based either on steric (repulsive) forces within the $Fe(CO)_4$ moiety or electronic (attractive) interactions between the carbonyl groups and the next metal center, as well as differing ionicity of the Fe−M bonds and packing interactions. As a matter of fact the bending of COs is present whenever **I**−**V** is bound to a sterically unhindered center and the amount of bending strongly depends on the electronegativity of the bonded atom (the lower the electronegativity the more pronounced the bending). This is well documented for group 15 derivatives. As reported in Figure 3, both the axial and the equatorial C−Fe−C bond angles decrease on moving from P to Bi, i.e. from the most to the least electronegative bonded atom. The importance of the Fe−X bond polarity, in determining the geometry of the $Fe(CO)_4$ fragment, was recognized by Hoffmann and co-workers,[23] and more recently CO bending in the $[(PtCO)_3\{\mu_2\text{-}Fe(CO)_4\}_3]^{n-}$ (n = 0, 1, 2) complexes has been attributed by Mealli to a d^{10} configuration of iron,[24] *i.e.* to the (formal) presence of $[Fe(CO)_4]^{2-}$ fragments. Indeed extended Hückel computations[25] on *cis*-$Fe(CO)_4X_2$ conformers, with different CO bending, clearly show that on decreasing the electronegativity of the X atoms (treated as pseudo H atoms, i.e. pure σ donors) the bending of the axial COs increases (see Figure 4). The minima of the total energy (continuous lines in

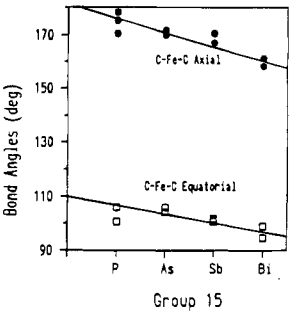

Figure 3. Plot of C_{ax}−Fe−C_{ax} and C_{eq}−Fe−C_{eq} bond angles found in *cis*-$Fe(CO)_4X_2$ fragments (X = group 15 element) extracted from the CSD. (Cambridge Structural Database): X = P, [CEGHEB] Flynn, K. M.; Hope, H.; Murray, B. D.; Olmstead, M. M.; Power, P. P.; *J. Am. Chem. Soc.* **1983**, *105*, 7570, [FALFUT] Mathieu, R.; Caminade, A.-M.; Majoral, J.-P.; Attali, S.; Sanchez, M. *Organometallics* **1986**, *5*, 1914, [GALVIY] del Pozo, A. G.; Caminade, A.-M.; Dahan, F.; Majoral, J.-P.; Mathieu, R.; *J. Chem. Soc., Chem. Commun.* **1988**, 574; X = As, [BZASFE] Jacob, M.; Weiss, E. *J. Organomet. Chem.* **1978**, *153*, 31, [CASFEM] Langenbach, H.-J.; Rottinger, E.; Vahrenkamp, H. *Chem. Ber.* **1980**, *113*, 42; X = Sb, [COXVAM] Cowley, A. H.; Norman, N. C.; Pakulsky, M.; Bricker, D. L.; Russell, D. H. *J. Am. Chem. Soc.* **1985**, *107*, 8211; X = Bi, [JASPIC] Whitmire, K. H.; Shieh, M.; Cassidy, J. *Inorg. Chem.* **1989**, *28*, 3164, [JIWTEO/JIWTAK] Cassidy, J.; Whitmire, K. H. *Inorg. Chem.* **1991**, *30*, 2788.

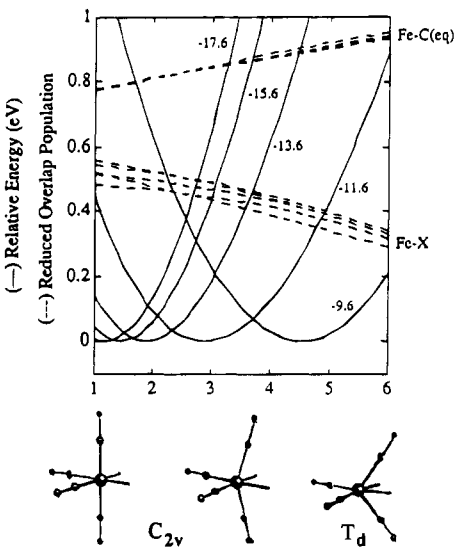

Figure 4. Total energies relative to the most stable conformer (continuous lines, eV) and selected (Fe−X and Fe−C_{eq}) reduced overlap populations (ROP, dashed lines) for *cis*-$Fe(CO)_4X_2$ on varying the local symmetry of the four CO ligands from C_{2v} to T_d and the VOIP of X atom from −17.6 to −9.6 eV.

Figure 4) shift to the right on varying the valence orbital ionization potential (VOIP) of the X atoms from −17.6 to −9.6 eV (i.e. decreasing the elettronegativity of the X atoms). Moreover, whatever the VOIP of the X atom, CO bending is associated with a decrease of the Fe−X and an increase of the Fe−C_{eq} reduced overlap populations (ROP, dashed lines in Figure 4). That is: strengthening of the Fe−C_{eq} bonds occurs at the expense of the Fe−X ones. When the bending of equatorial COs (from 90° to 109.4°) is analyzed separately from the axial ones (from 180 to 109.4°), it is evident that a lowering of the electronegativity favors the opening of the equatorial and the closure of the axial angles. However, at variance with these findings, the experimental data reported in Figure 3 show an opposite trend for the equatorial angles (at least for the P−Bi derivatives). Even so, the energy involved in equatorial bending is computed to be much lower (ca. $^1/_5$) than that for the axial bending. Analogously ROP curves are flat along the equatorial

(21) Longoni, G.; Manassero, M.; Sansoni, M. *J. Am. Chem. Soc.* **1980**, *102*, 3242.
(22) Ceriotti, A.; Brivio, E.; Heaton, B. T. Work in progress.
(23) Elian, M; Hoffmann, R.; *Inorg. Chem.* **1975**, *14*, 1058. Hoffmann, R.; Howell, J. M.; Rossi, A.; Wan,R. *J. Am. Chem. Soc.* **1976**, *98*, 2484.
(24) Mealli, C. *J. Am. Chem. Soc.* **1985**, *107*, 2245.
(25) Hoffmann, R. *J. Chem. Phys.* **1963**, *39*, 1397. Hoffmann, R.; Lipscomb, W. N. *J. Chem. Phys.* **1962**, *36*, 3489. Hoffmann,R.; Lipscomb, W. N. *J. Chem. Phys.* **1962**, *37*, 2872.

distorsion. Thus, it is relatively simple to conclude that the bending of the equatorial COs can be easily overcome by steric effects (Bi is larger than P).

Moreover, it is important to note that the amount of CO bending does not affect the number of electrons which the fragment makes available for donation. Thus, **VI** donates two electrons irrespective of the amount of "tetrahedricity" and bond polarity. In fact, even when, at the limiting T_d symmetry, the frontier orbitals are triply degenerate and contain four electrons, only two of them have the proper symmetry to interact with the incoming ligands in a *cis*-(face)bicapped geometry.

The above considerations may be summarized by saying that the $Fe(CO)_4$ fragments do not distort in order to "augment" their "formal" donor capabilities (in order to fulfill some cluster electron requirements) or to strengthen the $M-Fe(CO)_4$ interactions. The bending probably occurs to stabilize the individual $Fe(CO)_4$ fragments both through a release of repulsive as well as a gain in attractive electronic energy within the moiety. Unhindered late transition M atoms do not oppose such distortions, which may be even enhanced and progressively stabilized by long range C···M attractive interactions. Because the bending of the axial COs stabilizes the $Fe(CO)_4$ fragments more than the bending of the equatorial ones, it is common to observe these distortions in those "raft" clusters where crowding is concentrated on the equatorial plane while the axial ligands are sterically free.

Bearing in mind this behavior of the d^8 $M(CO)_4$ fragments, we can analyze the bonding and attempt a rationalization of the chemistry of the title Ag−Fe clusters. Here, we report some pertinent cluster geometries and their computed CVEs numbers, assuming that all the metal centers reach 18 electrons (excepting the interstitial atom) and all the edges correspond to two-center−two-electron bonds. $[Ag_4\{\mu_2\text{-}Fe(CO)_4\}_4]^{4-}$ has 112 CVEs and can be reasonably related to cluster **A** which is expected to have 128 CVEs when all the valence orbitals are "active"; however, when eight valence orbitals are inoperative, *i.e.* if the four radial and four out-of-plane Ag p orbitals are considered high energy (empty) noninteracting orbitals, cluster **A** has only 112 CVEs. On the other hand, if the radial p orbitals were strongly contributing to Ag−Ag bonds, $[Ag_4\{\mu_2\text{-}Fe(CO)_4\}_4]^{4-}$ could be equally well related to cluster **B** (120 CVEs), which is expected to have 112 CVEs when four out-of-plane p orbitals are left empty.

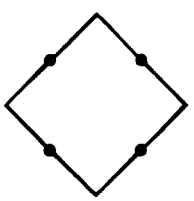

A 128

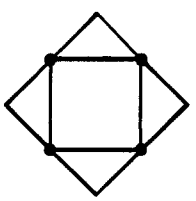

B 120

$[Ag_4\{\mu_2\text{-}Fe(CO)_4\}_4]^{4-}$ can also be considered as an Ag_4 cluster (56 CVEs) stabilized by four $Fe(CO)_4$ ligands of type **II** or **VI**. Depending on the assumed number (eight or four) of inoperative p orbitals, it can be related either to **C** or **D** (72 and 64 CVEs, respectively).[26]

The electron bookkeeping of $[Ag_5\{\mu_2\text{-}Fe(CO)_4\}_2\{\mu_3\text{-}Fe(CO)_4\}_2]^{3-}$ (122 CVEs) is as ambiguous as that of $[Ag_4\{\mu_2\text{-}Fe(CO)_4\}_4]^{4-}$. In fact, $[Ag_5\{\mu_2\text{-}Fe(CO)_4\}_2\{\mu_3\text{-}Fe(CO)_4\}_2]^{3-}$ can be related either to **E**, under the assumption of 10 inoperative Ag p orbitals, or to a nonbonded Ag_5 cluster (**F**), stabilized by two μ_2-$Fe(CO)_4$ ligands of type **II** and two four-electron donor μ_3-$Fe(CO)_4$ ligands of type **IV**.

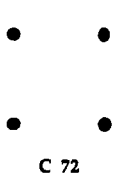

C 72

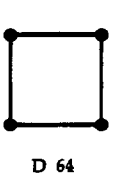

D 64

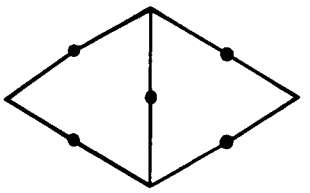

E 142

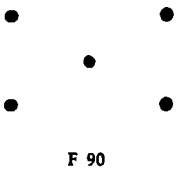

F 90

The correlation with **G** or **H**, however, is possible only in a very formal way, because one is forced to assume that all the radial p orbitals are operative and only four out of five out-of-plane p orbitals are inoperative, which is difficult to justify. In-plane hexacoordination appears to be inconsistent with the EAN rule, i.e. the six in-plane interactions at the central Ag atoms cannot be considered as two-center−two-electron bonds.

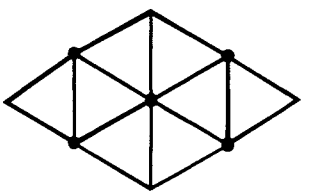

G 130

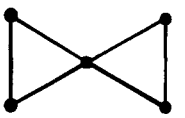

H 78

Alternatively, the "observed" CVE number can be rationalized by considering the central Ag atom to be "interstitial". The flattening along one of the two diagonals of **A** to give **I** will cost some energy but no bond-breaking, due to the lack of Ag−Ag bonds in **A**; therefore, **A** and its distorted version **I** must share the same CVE number. The addition of the interstitial Ag atom in **J** is associated with the presence of 10 more CVEs because, as recently reported,[30] the five (contracted and low-energy) d orbitals of the interstitial Ag atom afford a narrow band of five more (filled) cluster valence orbitals. The above scheme obviously requires the presence of eight inoperative p orbitals and the corrected CVE number for **J** (138 − 16 = 122) coincides with that observed.

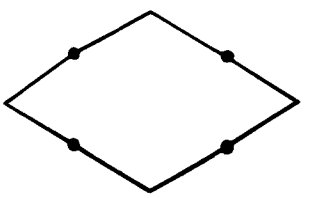

I (= A) 128

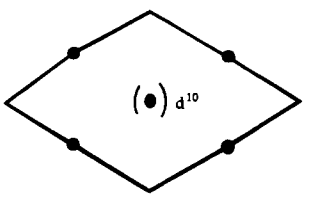

J 138

The above reasoning demonstrates that rationalization of a cluster electron count may become a matter of personal feeling. Many different schemes can afford the "correct" CVE number (which is not always uniquely defined), and this is not enough to grant some chemical insight in the underlying assumptions.

(26) Analogous conclusions can be drawn analyzing other known raft clusters such as $[Cu_3\{Fe(CO)_4\}_3]^{3-}$ [13] and $[Pt_3\{Fe(CO)_4\}_3(CO)_3]^{n-}$ [27-29] in similar terms.

(27) Longoni, G.; Manassero, M.; Sansoni, M. *J. Am. Chem. Soc.* **1980**, *102*, 7973.
(28) Adams,R. C.; Chen, G.; Wang, J. G. *Polyhedron* **1989**, *8*, 2521.
(29) Della Pergola, R.; Garlaschelli, L.; Mealli, C.; Proserpio, D. M.; Zanello, P.; *J. Cluster Sci.* **1990**, *1*, 93.
(30) Sironi, A. *J. Chem. Soc., Dalton Trans.* **1993**, 173.

Better insight can be obtained by qualitative MO calculations. Extended Huckel computations on $[Ag_4\{\mu_2\text{-}Fe(CO)_4\}_4]^{4-}$ and $[Ag_5\{\mu_2\text{-}Fe(CO)_4\}_2\{\mu_3\text{-}Fe(CO)_4\}_2]^{3-}$ clearly show that periferal Ag atoms are essentially two coordinated to Fe and that the central Ag atom interacts with all six nearest metals even if the strongest interactions are those with the two Fe atoms. There is a mixing of 5s and (radial) 5p into 4d orbitals converting repulsive $d^{10}\cdots d^{10}$ (Ag−Ag) interactions into partial bonding (such mixing was previously shown to occur in several Cu clusters and has been used to interpret unexpectedly short Cu−Cu contacts[31]). The out-of-plane Ag orbitals are also involved in long-range interactions with the axial CO ligands. Nevertheless, as far as electron bookkeeping is concerned, the radial and out-of-plane Ag p orbitals must be essentially considered as empty, high energy, noninteracting orbitals; hence, $[Ag_4\{\mu_2\text{-}Fe(CO)_4\}_4]^{4-}$ is most closely related to cluster **A**, whereas $[Ag_5\{\mu_2\text{-}Fe(CO)_4\}_2\{\mu_3\text{-}Fe(CO)_4\}_2]^{3-}$ is better related to **E** or **J**.

Conclusions

The MO analysis reported in the previous section not only nicely rationalizes the chemistry of $Ag-Fe(CO)_4$ and related clusters isolated to date, but it also suggests future experiments. First of all, the two $Fe(CO)_4$ fragments of the linear $[M\{Fe(CO)_4\}_2]^{n-}$ (M = Ag, n = 3; M = Zn, Cd, Hg, n = 2)[10,11] trinuclear clusters, on rearrangement from **I** to **VI** stereogeometries, make two outpointing filled orbitals available; hence the cluster becomes a bidentate four-electron ligand formally comparable to bis(diphenylphosphino)methane (dppm). As a consequence, the reaction of $[Ag\{Fe(CO)_4\}_2]^{3-}$ with 1 mol of Ag^+ to give $[Ag_4\{\mu_2\text{-}Fe(CO)_4\}_4]^{4-}$, as well as the corresponding reactions of $[M\{Fe(CO)_4\}_2]^{2-}$ with M^{2+} to give $[M_4\{Fe(CO)_4\}_4]$ (M = Cd, Hg),[32] are strictly comparable to the formation of $[Au_2(dppm)_2Cl_2]$ from AuCl and dppm.[33]

Similarly, **VI** can easily transform into **IV**, making $[Ag_4\{\mu_2\text{-}Fe(CO)_4\}_4]^{4-}$ potentially a pseudo 8-crown-4 ligand as the iron centers have four extra filled orbitals available for in-plane interactions at the center of the square with an incoming atom or ion on widening the four Ag−Fe−Ag angles. Such a deformation will result in loss of linearity of silver as the Fe−Ag−Fe angle departs from 180°. Therefore, the most likely alternative consists in the widening of only two Ag−Fe−Ag angles (and the corresponding elongation of only two out of four Ag−Ag contacts), giving rise to a pseudo 8-crown-2 ligand.[34] This second possibility is nicely illustrated by the structure of $[Ag_5\{\mu_2\text{-}Fe(CO)_4\}_2\{\mu_3\text{-}Fe(CO)_4\}_2]^{3-}$, which can be envisioned as a Ag^+ complex of the $[Ag_4\{\mu_2\text{-}Fe(CO)_4\}_4]^{4-}$ 8-crown-2 ligand. This interpretation of $[M_5\{\mu_2\text{-}Fe(CO)_4\}_2\{\mu_3\text{-}Fe(CO)_4\}_2]^{3-}$ (M = Cu, Ag), which requires weak M−M interactions, implies that the concerted cross engagement and disengagement of the iron bites with the central ion should be relatively easy and would be in keeping with the equivalence of the carbonyl groups of the two nonequivalent $Fe(CO)_4$ fragments found experimentally in $[Cu_5\{\mu_2\text{-}Fe(CO)_4\}_2\{\mu_3\text{-}Fe(CO)_4\}_2]^{3-}$ by ^{13}C and ^{17}O NMR.[35]

As a result of the above picture of the Ag−Fe and Cu−Fe clusters, the designed synthesis of some other pseudo dppm or pseudo-8-crown-2 cluster−ligand complexes, from $[M\{Fe(CO)_4\}_2]^{n-}$ and $[M_4\{\mu_2\text{-}Fe(CO)_4\}_4]^{n-}$, respectively, could be anticipated.

Finally, it appears conceivable to conclude that formation of an $[M_4\{\mu_2\text{-}Fe(CO)_4\}_4]^{4-}$ species in the case of silver, rather than an $[M_3\{\mu_2\text{-}Fe(CO)_4\}_3]^{3-}$ oligomer as for copper, is mainly due to thermodynamic reasons. Thus, an idealized bridged square implies M−M contacts ca. 40% longer than the Fe−M distances, whereas the triangle of frequency 2 requires equal Fe−M and M−M interatomic separations. The longer Ag−Ag distances in comparison to the Fe−Ag interaction, as well as the closer Fe−Cu and Cu−Cu values, make the adoption of the two above differing structures understandable. In both cases, the opposite choice would have only been possible through a greater departure of the Fe−M−Fe angle from 180° and at the expense of some Fe−M bonding energy. As clearly shown by our EHMO calculations on the Ag−Fe clusters, as well as recent Fenske−Hall calculations on the Cu−Fe clusters,[36] Fe−M bonds show an overlap population much greater than the M−M interactions and their strength is at the origin of the existence of these clusters.

Experimental Section

All reactions including sample manipulations were carried out using standard Schlenk techniques under nitrogen and in carefully dried solvents. The $Na_2[Fe(CO)_4]\cdot x$THF ($x \sim 2$) salt was prepared according to the literature.[37] Analyses of Fe and Ag were performed by atomic absorption on a Pye-Unicam instrument and gravimetrically as BPh_4^- salts for the tetrasubstituted ammonium cations. Infrared spectra were recorded on a Perkin Elmer 1605 interferometer using CaF_2 cells.

1. Synthesis of $[Na(15\text{-crown-}5)]_3[AgFe_2(CO)_8]$. Solid $AgNO_3$ (0.4 g, 2.35 mmol) was added in portions over a period of 2 h to a stirred suspension of $Na_2[Fe(CO)_4]\cdot x$THF (1.78 g, 4.97 mmol for x = 2) in thf (20 cm^3) containing 15-crown-5 (2.1 g, 9.5 mmol). The resulting white precipitate of $[Na(15\text{-crown-}5)]_3[AgFe_2(CO)_8]$ was filtered and dried in vacuum. The solid may contain trace amounts of $[HFe(CO)_4]^-$ as impurity. Anal. Calcd for $[Na(15\text{-crown-}5)]_3[AgFe_2(CO)_8]$: Ag, 9.20; Fe, 9.53. Found: Ag,8.91; Fe, 9.71.

2. Synthesis of $[Na(15\text{-crown-}5)]_4[Ag_4Fe_4(CO)_{16}]$ from $Na_2[Fe(CO)_4]\cdot x$THF. Solid $AgNO_3$ (1.2 g, 7.06 mmol) was added in portions over a period of 2 h to a stirred suspension of $Na_2[Fe(CO)_4]\cdot x$THF (2.71 g, 7.57 mmol for x = 2) in THF (40 cm^3). The resulting yellow-orange suspension was filtered and 15-crown-5 (1.7 g) was added with stirring to the solution. The resulting pale yellow precipitate of $[Na(15\text{-crown-}5)]_4[Ag_4Fe_4(CO)_{16}]$ was filtered and dried under vacuum. Anal. Calcd for $[Na(15\text{-crown-}5)]_4[Ag_4Fe_4(CO)_{16}]$: Ag, 20.80; Fe, 10.77. Found: Ag,20.25; Fe, 10.54.

3. Synthesis of $[NMe_3CH_2Ph]_4[Ag_4Fe_4(CO)_{16}]$ from $[NMe_3CH_2Ph]_3[Ag_5Fe_4(CO)_{16}]$. Solid $Na_2[Fe(CO)_4]\cdot x$THF (0.72 g, 2 mmol) was added under stirring to a solution of $[NMe_3CH_2Ph]_3[Ag_5Fe_4(CO)_{16}]$ (2.4 g, 1.45 mmol) in CH_3CN (40 cm^3), and the formation of $[Ag_4Fe_4(CO)_{16}]^{4-}$ was monitored by IR. The resulting yellow-orange solution was dried in vacuum. The residue was washed with two portions of THF (10 cm^3), dissolved in CH_3CN (20 cm^3), and layered with diisopropyl ether. Then 0.87 g of well-shaped pale yellow crystals of $[NMe_3CH_2Ph]_4[Ag_4Fe_4(CO)_{16}]$ separated out in 2 days. Anal. Calcd for $[NMe_3CH_2Ph]_4[Ag_4Fe_4(CO)_{16}]$: $NMe_3CH_2Ph^+$, 35.23; Ag, 25.34; Fe, 13.12]. Found: $NMe_3CH_2Ph^+$, 34.74; Ag, 25.01;Fe, 12.94.The $[NEt_4]_4[Ag_4Fe_4(CO)_{16}]$ and $[N(PPh_3)_2]_4[Ag_4Fe_4(CO)_{16}]$ salts have been similarly prepared on starting from the corresponding $[Ag_5Fe_4(CO)_{16}]^{3-}$ salts.

4. Synthesis of $[NMe_3CH_2Ph]_3[Ag_5Fe_4(CO)_{16}]$ from $Na_2[Fe(CO)_4]\cdot x$THF. Solid $AgNO_3$ (1.70 g, 10 mmol) was added in portions to a stirred solution of $Na_2[Fe(CO)_4]\cdot x$THF (2.84 g, 7.94 mmol for x =

(31) Merz, K. M.; Hoffmann, R. *Inorg. Chem.* **1988**, *27*, 2120.
(32) Ernst, R. D.; Marks, T. J.; Ibers, J. A. *J. Am. Chem. Soc.* **1977**, *99*, 2090.
(33) Hall, K. P.; Mingos, D. M. P. *Prog. Inorg. Chem.* **1984**, *32*, 237.
(34) A snapshot of such a distortion is represented by the second modification of the $[Au_4\{Fe(CO)_4\}_4]^{4-}$ recently found on determining the solid state structure of $[NEt_4]_4[Au_4\{Fe(CO)_4\}_4]$; Albano, V. G.; Calderoni, F.; Iapalucci, M. C.; Longoni, G.; Monari, M. Manuscript in preparation.
(35) Doyle, G.; Heaton, B. T.; Occhiello, E. *Organometallics*, **1985**, *4*, 1224.
(36) Buhl, M. L.; Long, G. J.; Doyle, G. *J. Organomet. Chem.* **1993**, *461*, 187.
(37) Collman, J. P.; Finke, R. G.; Cawse, J. N.; Brauman, J. I. *J. Am. Chem. Soc.* **1977**, *99*, 2515.

Table 3. Crystal Data for $[NMe_3CH_2Ph]_4[Ag_4\{\mu_2\text{-}Fe(CO)_4\}_4]$ and $[NEt_4]_3[Ag_5\{\mu_2\text{-}Fe(CO)_4\}_2\{\mu_3\text{-}Fe(CO)_4\}_2]$[a]

complex	$[NMe_3CH_2Ph]_4[Ag_4Fe_4(CO)_{16}]$	$[NEt_4]_3[Ag_5Fe_4(CO)_{16}]$
formula	$C_{56}H_{64}Ag_4Fe_4N_4O_{16}$	$C_{40}H_{60}Ag_5Fe_4N_3O_{16}$
fw	1704.02	1601.67
cryst size, mm	0.20 × 0.20 × 0.30	0.15 × 0.20 × 0.45
cryst syst	monoclinic	tetragonal
space group	$P2_1/n$ (No. 14)	$P4_2/mnm$ (No. 136)
a, Å	11.419(4)	14.004(1)
b, Å	29.714(5)	14.004(1)
c, Å	19.227(3)	14.278(1)
β, deg	92.40(2)	
V, Å^3	6517.8	2800.3
Z	4	2
D_{calcd}, g cm^{-3}	1.74	1.90
no. of reflcns collcd	5360 ($\pm h,+k,+l$)	3544 ($+h,+k,+l$)
no. of unique obsd reflcns [$F_o > 4\sigma(F_o)$]	3182	1187
μ(Mo Kα), cm^{-1}	21.27	27.49
R,[b] R_w[c]	0.035, 0.036	0.039, 0.044
quality-of-fit-indicator[d]	1.45	0.73

[a] Radiation (graphite monochromated), Mo Kα (0.710 67 Å); temperature, 295−298 K. [b] $R = \Sigma||F_o| - |F_c||/\Sigma|F_o|$. [c] $R_w = [\Sigma w(|F_o| - |F_c|)^2/\Sigma w|F_o|^2]^{1/2}$. [d] Quality-of-fit = $[\Sigma w(F_o - F_c)^2/(N_{obs} - N_{par})]^{1/2}$.

Table 4. Fractional Atomic Coordinates (Å) with Esd's in Parentheses for $[NMe_3CH_2Ph]_4$ $[Ag_4Fe_4(CO)_{16}]$

atom	x	y	z	atom	x	y	z
Ag(1)	0.47565(9)	0.19102(3)	0.26071(5)	C(18)	0.4803(11)	0.2199(4)	0.7271(7)
Ag(2)	0.69686(9)	0.11982(3)	0.23915(5)	C(19)	0.3310(11)	0.1643(4)	0.7434(6)
Ag(3)	0.67027(9)	0.13376(3)	0.08287(5)	C(20)	0.5181(10)	0.1431(3)	0.6915(6)
Ag(4)	0.46845(9)	0.20543(3)	0.10354(5)	C(21)	0.4777(7)	0.0994(2)	0.6590(4)
Fe(1)	0.34594(15)	0.24858(5)	0.19157(9)	C(22)	0.4870(7)	0.0926(2)	0.5877(4)
Fe(2)	0.58773(15)	0.14041(5)	0.34942(9)	C(23)	0.4533(7)	0.0516(2)	0.5579(4)
Fe(3)	0.83191(15)	0.08641(5)	0.14798(9)	C(24)	0.4104(7)	0.0173(2)	0.5994(4)
Fe(4)	0.54283(14)	0.17448(4)	−0.01135(8)	C(25)	0.4012(7)	0.0242(2)	0.6708(4)
C(1)	0.2788(11)	0.1952(3)	0.1836(7)	C(26)	0.4348(7)	0.0652(2)	0.7006(4)
O(1)	0.2282(8)	0.1607(3)	0.1768(5)	N(2)	0.7459(8)	−0.0003(2)	0.8647(5)
C(2)	0.2946(12)	0.2714(4)	0.2690(6)	C(27)	0.6818(12)	−0.0036(4)	0.9290(7)
O(2)	0.2598(10)	0.2875(4)	0.3191(6)	C(28)	0.8543(12)	0.0261(4)	0.8799(8)
C(3)	0.2734(12)	0.2787(4)	0.1243(7)	C(29)	0.7776(11)	−0.0468(4)	0.8430(7)
O(3)	0.2184(11)	0.2984(3)	0.0818(6)	C(30)	0.6660(10)	0.0230(3)	0.8096(6)
C(4)	0.4897(10)	0.2705(4)	0.1902(7)	C(31)	0.7213(6)	0.0375(2)	0.7451(3)
O(4)	0.5791(9)	0.2890(3)	0.1939(6)	C(32)	0.7172(6)	0.0088(2)	0.6876(3)
C(5)	0.4911(12)	0.1560(4)	0.4131(7)	C(33)	0.7581(6)	0.0236(2)	0.6242(3)
O(5)	0.4265(9)	0.1650(5)	0.4562(6)	C(34)	0.8032(6)	0.0670(2)	0.6182(3)
C(6)	0.6820(11)	0.1055(4)	0.3983(8)	C(35)	0.8073(6)	0.0957(2)	0.6757(3)
O(6)	0.7447(9)	0.0818(3)	0.4313(6)	C(36)	0.7664(6)	0.0809(2)	0.7391(3)
C(7)	0.5011(11)	0.1038(4)	0.2969(7)	N(3)	1.0861(8)	0.1559(2)	0.3692(5)
O(7)	0.4366(9)	0.0791(3)	0.2682(6)	C(37)	1.1754(11)	0.1216(4)	0.3480(7)
C(8)	0.6767(10)	0.1876(4)	0.3303(7)	C(38)	1.0267(11)	0.1742(4)	0.3051(7)
O(8)	0.7365(8)	0.2187(3)	0.3199(5)	C(39)	1.1501(10)	0.1919(3)	0.4084(6)
C(9)	0.9054(11)	0.0619(4)	0.2208(6)	C(40)	0.9940(10)	0.1339(3)	0.4114(6)
O(9)	0.9557(10)	0.0460(3)	0.2682(5)	C(41)	1.0371(6)	0.1111(2)	0.4770(3)
C(10)	0.9137(11)	0.0674(4)	0.0787(6)	C(42)	1.0647(6)	0.0654(2)	0.4744(3)
O(10)	0.9717(10)	0.0558(3)	0.0338(5)	C(43)	1.1060(6)	0.0431(2)	0.5344(3)
C(11)	0.6994(10)	0.0553(4)	0.1377(8)	C(44)	1.1198(6)	0.0666(2)	0.5971(3)
O(11)	0.6217(8)	0.0305(3)	0.1270(6)	C(45)	1.0922(6)	0.1123(2)	0.5997(3)
C(12)	0.8692(11)	0.1437(3)	0.1486(7)	C(46)	1.0509(6)	0.1345(2)	0.5397(3)
O(12)	0.9066(7)	0.1810(3)	0.1514(5)	N(4)	0.0428(8)	0.1895(3)	−0.0429(5)
C(13)	0.6548(10)	0.2115(3)	0.0172(6)	C(47)	−0.0685(10)	0.1622(4)	−0.0482(7)
O(13)	0.7296(8)	0.2376(3)	0.0289(5)	C(48)	0.1170(12)	0.1737(4)	0.0157(7)
C(14)	0.4431(11)	0.2116(4)	−0.0498(8)	C(49)	0.0101(12)	0.2373(4)	−0.0318(8)
O(14)	0.3801(10)	0.2366(4)	−0.0778(8)	C(50)	0.1076(10)	0.1865(3)	−0.1112(6)
C(15)	0.4585(10)	0.1325(4)	0.0259(7)	C(51)	0.1311(6)	0.1403(2)	−0.1360(3)
O(15)	0.3956(9)	0.1042(3)	0.0443(6)	C(52)	0.2277(6)	0.1170(2)	−0.1075(3)
C(16)	0.5959(15)	0.1449(4)	−0.0808(8)	C(53)	0.2523(6)	0.0737(2)	−0.1307(3)
O(16)	0.6334(17)	0.1255(4)	−0.1269(7)	C(54)	0.1804(6)	0.0537(2)	−0.1823(3)
N(1)	0.4244(7)	0.1786(2)	0.6954(4)	C(55)	0.0838(6)	0.0770(2)	−0.2108(3)
C(17)	0.3726(12)	0.1896(4)	0.6272(7)	C(56)	0.0591(6)	0.1203(2)	−0.1876(3)

2) in CH_3CN (30 cm^3) over a period of 4 h. The resulting dark suspension was evaporated in vacuum to dryness, and the residue was suspended in methanol and filtered. The methanol solution was precipitated by addition of solid $[NMe_3CH_2Ph]Br$. The resulting solid material was washed several times with water and dried. The remaining precipitate was dissolved in acetone (30 cm^3) and precipitated by slow diffusion of isopropyl alcohol (40 cm^3) to give 3.57 g of well-shaped pale yellow crystals of $[NMe_3CH_2Ph]_3[Ag_5Fe_4(CO)_{16}]$. These are soluble in acetone and acetonitrile, less soluble in THF, and insoluble in nonpolar solvents. Anal. Calcd for $[NMe_3CH_2Ph]_3[Ag_5Fe_4(CO)_{16}]$: $NMe_3CH_2Ph^+$, 27.10; Ag, 32.48; Fe, 13.45. Found: $NMe_3CH_2Ph^+$, 26.81; Ag, 31.95; Fe, 13.24. The corresponding $[NEt_4]^+$ and $[N(PPh_3)_2]^+$ salts have been similarly prepared and crystallized either from acetone−isopropyl alcohol or acetonitrile−diisopropyl ether.

5. X-ray Data Collection and Crystal Structure Determination for $[NMe_3CH_2Ph]_4[Ag_4\{\mu_2\text{-}Fe(CO)_4\}_4]$ and $[NEt_4]_3[Ag_5\{\mu_2\text{-}Fe(CO)_4\}_2\{\mu_3\text{-}Fe(CO)_4\}_2]$. Single crystals of both $[NMe_3CH_2Ph]_4[Ag_4\{\mu_2\text{-}Fe(CO)_4\}_4]$ and $[NEt_4]_3[Ag_5\{\mu_2\text{-}Fe(CO)_4\}_2\{\mu_3\text{-}Fe(CO)_4\}_2]$ were

Table 5. Fractional Atomic Coordinates (Å) with Esd's in Parentheses for $[NEt_4]_3[Ag_5Fe_4(CO)_{16}]$

atom	*x*	*y*	*z*
Ag(1)	0.00000	0.00000	0.00000
Ag(2)	0.04266(4)	0.19498(3)	0.00000
Fe(1)	0.13769(6)	−0.13769(6)	0.00000
Fe(2)	0.22480(6)	0.22480(6)	0.00000
C(1)	0.2640(5)	−0.1328(6)	0.0000
O(1)	0.3469(4)	−0.1392(7)	0.0000
C(2)	0.3919(3)	0.3919(3)	0.6171(5)
O(2)	0.4067(3)	0.4067(3)	0.6956(4)
C(3)	0.3471(6)	0.2062(5)	0.0000
O(3)	0.4325(5)	0.1943(5)	0.0000
C(4)	0.1956(4)	0.1956(4)	−0.1155(6)
O(4)	0.1838(4)	0.1838(4)	−0.1961(4)
N(1)	0.00000	0.50000	0.25000
C(5)	0.0276(7)	0.5829(5)	0.3148(6)
C(5A)	0.0785(11)	0.4669(13)	0.3144(8)
C(6)	0.0527(6)	0.6735(5)	0.2601(6)
N(2)	0.00000	0.00000	0.50000
C(7)	0.0815(11)	−0.0014(9)	0.4376(11)
C(8)	0.0958(9)	0.0958(9)	0.3787(9)

sealed inside thin-walled glass capillaries. Crystal data for both species are given in Table 3. The diffraction experiments were carried out at room temperature on a fully automated Enraf-Nonius CAD4 diffractometer. The cell dimensions were determined from 25 randomly selected strong reflections by using automatic search, indexing, and least-squares routines. Intensity data were corrected for Lorentz and polarization effects. Three check reflections, monitored periodically during data collection, revealed a total loss of intensity of 32% and 40% for $[NMe_3CH_2Ph]_4[Ag_4\{\mu_2\text{-}Fe(CO)_4\}_4]$ and $[NEt_4]_3[Ag_5\{\mu_2\text{-}Fe(CO)_4\}_2\{\mu_3\text{-}Fe(CO)_4\}_2]$, respectively, and the decay was corrected accordingly. An empirical absorption correction was applied on both crystals by using the azimuthal scan method.[38] All calculations were performed by using the SHELX 76 package of programs.[39] The metal atom positions were determined by direct methods and all non hydrogen atoms located from difference-Fourier syntheses. $[NEt_4]_3[Ag_5\{\mu_2\text{-}Fe(CO)_4\}_2\{\mu_3\text{-}Fe(CO)_4\}_2]$ was directly refined in the space group $P4_2/mnm$ (No. 136), taking advantage of the ascertained isomorphism with the copper analogue $[NEt_4]_3[Cu_5\{\mu_2\text{-}Fe(CO)_4\}_2\{\mu_3\text{-}Fe(CO)_4\}_2]$.[13] The anions $[Ag_5\{\mu_2\text{-}Fe(CO)_4\}_2\{\mu_3\text{-}Fe(CO)_4\}_2]^{3-}$ were found placed around the special position *a* of site symmetry D_{2h} (*mmm*). One cation [N(1)] was found placed around the special positions *d* of S_4 (4) site symmetry (independent fraction $^2/_8$). The CH_2 groups were found disordered with sligthly uneven populations of the vertices of a cube centered at N(1). Another cation [N(2)] was found around the special position *b* of D_{2h} (*mmm*) site symmetry (independent fraction $^1/_8$). For this cation the CH_2 groups were obliged to be disordered with occupancy factor of 0.5. During the final refinement stages for $[NMe_3CH_2Ph]_4[Ag_4\{\mu_2\text{-}Fe(CO)_4\}_4]$ the atoms of the tetranion were treated anisotropically while the cation atoms were refined isotropically with the phenyl rings treated as rigid groups (C−C 1.395 Å; C−H 1.08 Å; C−C−C 120°) and the hydrogen atoms added in calculated positions. The refinement of positional and thermal parameters for $[NEt_4]_3[Ag_5\{\mu_2\text{-}Fe(CO)_4\}_2\{\mu_3\text{-}Fe(CO)_4\}_2]$ proceeded using anisotropic thermal parameters for all non hydrogen atoms. The final difference-Fourier maps showed residual peaks not exceeding 0.69 e Å^{-3} for $[NMe_3CH_2Ph]_4[Ag_4\{\mu_2\text{-}Fe(CO)_4\}_4]$ and 0.50 e Å^{-3} for $[NEt_4]_3[Ag_5\{\mu_2\text{-}Fe(CO)_4\}_2\{\mu_3\text{-}Fe(CO)_4\}_2]$. Positional parameters with their estimated standard deviations corresponding to the final least-squares calculations are given in Table 4 for $[NMe_3CH_2Ph]_4[Ag_4\{\mu_2\text{-}Fe(CO)_4\}_4]$ and in Table 5 for $[NEt_4]_3[Ag_5\{\mu_2\text{-}Fe(CO)_4\}_2\{\mu_3\text{-}Fe(CO)_4\}_2]$.

6. EHMO Computations. The computational procedure used was the Extended Hückel method,[25] with weighted H_{ij}'s,[40] within the FMO formalism,[41] using a local version of CACAO.[42] The molecular geometries were idealized using the following bond lengths: Fe−Ag, Fe−C, Fe−X(H), and C−O = 2.60, 1.80, 1.56, and 1.15 Å, respectively. $[Ag_4(Fe(CO)_4)_4]^{4-}$ and $[Ag_5(Fe(CO)_4)_4]^{3-}$ have been idealized to D_{4h} and D_{2h} symmetries, respectively, using the experimental averaged bond angles. The EHT parameters are the same as in ref 1.

Acknowledgment. We thank the EEC and the MURST for a grant.

Supplementary Material Available: Tables of atomic coordinates of all atoms, anisotropic and isotropic thermal parameters of all non-hydrogen atoms for $[NMe_3CH_2Ph]_4[Ag_4\{\mu_2\text{-}Fe(CO)_4\}_4]$ (Tables S1−S3) and $[NEt_4]_3[Ag_5\{\mu_2\text{-}Fe(CO)_4\}_2\{\mu_3\text{-}Fe(CO)_4\}_2]$ (Tables S4−S6) and full details of data collection (Table S7) (13 pages). Ordering information is given on any current masthead page.

(38) North, A. C.; Philips, D. C.; Mathews F. S. *Acta Crystallogr.* **1968**, *A24*, 351.
(39) Sheldrick, G. M. SHELX 76, Program for Crystal Structure Determination. University of Cambridge, 1976.
(40) Ammeter, J. H.; Burgi, H.-B.; Thibeault, J. C.; Hoffmann, R. *J. Am. Chem. Soc.* **1978**, *100*, 3686.
(41) Hoffmann, R.; Fujimoto, H.; Swenson, J. R.; Wan, C. C. *J. Am. Chem. Soc.* **1973**, *95*, 7644. Hoffmann, R.; Fujimoto, H. *J. Phys. Chem.*, **1974**, *78*, 1167.
(42) Mealli, C.; Proserpio, D. M. *J. Chem. Educ.* **1990**, *66*, 399.